The decay of the $^6I_{7/2}$ term level of Gd^{3+} in YOCl and $LiYF_4$

1990 J. Phys.: Condens. Matter 2 5171

(http://iopscience.iop.org/0953-8984/2/23/007)

J. Phys.: Condens. Matter 2 (1990) 5171–5178. Printed in the UK

The decay of the $^6I_{7/2}$ term level of Gd^{3+} in YOCl and $LiYF_4$

J Sytsma, G F Imbusch† and G Blasse

Debye Research Institute, University of Utrecht, PO Box 80000, 3508 TA Utrecht, The Netherlands

Received 19 December 1989, in final form 5 March 1990

Abstract. The total decay rate of the $^6I_{7/2}$ term level of Gd^{3+} in YOCl and $LiYF_4$ is studied as a function of temperature. This rate is described as a thermal average of the different contributions of the crystal field components. The difference between the rates in YOCl and $LiYF_4$ is discussed.

1. Introduction

Dopant rare earth (RE) ions are well known for their luminescence properties. Transitions between $4f^7$ electronic levels of RE ions are characterised by sharp line emissions and long decay times. These characteristics make the RE ion very suitable for practical applications, such as in fluorescent lamp phosphors [1,2], colour television tubes [1], and laser materials [3].

The interaction of the $4f^7$ electrons of the RE ion with the host lattice is weak, because the 4f electrons are shielded from the environment by the $5s^2$ and $5p^6$ electrons.

Non-radiative transition rates within the $4f^7$ configuration have been investigated by many authors [4]. Rules exist for estimating non-radiative decay rates across the energy gap between the different term levels [4]. Crystal field splitting of the term levels is not taken into account in this analysis. Non-radiative decay rates from the different crystal field levels will, in general, be different, and the overall decay rate from a term level is a thermal average over the different crystal field levels.

In the case of Gd^{3+} it is possible to separate these contributions with high resolution laser spectroscopy. To show this, we determined the temperature dependence of the decay rate of the $^6I_{7/2}$ term level of Gd^{3+} in YOCl and extended earlier considerations on the decay rate of Gd^{3+} in $LiYF_4$ [5].

2. Theoretical description

An excited rare earth ion in a solid has different pathways to the ground state. Radiative and non-radiative decay and depopulation via energy migration [6] are the most important ones. The influences of energy migration can be suppressed by taking a low concentration of optically active ions.

† Permanent address: Deptartment of Physics, University College, Galway, Ireland.

0953-8984/90/235171+08$03.50

In this case the total decay rate of an initial energy level $|i\rangle$ is given by

$$A_d(T) = \sum_f A_r(|i\rangle \rightarrow |f\rangle) + \sum_{f'} A_{nr}(|i\rangle \rightarrow |f'\rangle) \tag{1}$$

where A_r and A_{nr} refer to radiative and non-radiative decay rates, respectively. The summation over $|f\rangle$ is over all energy levels to which $|i\rangle$ decays radiatively. The summation over $|f'\rangle$ is over those levels to which $|i\rangle$ decays non-radiatively. The radiative transition consists of a pure electronic transition (zero-phonon line) and vibronic transitions

$$A_r = A_{zp} + A_{vib}. \tag{2}$$

The pure electronic transition rate A_{zp} has, in general, both a forced electric dipole (FED) and a magnetic dipole (MD) contribution. The first can be expressed in terms of three parameters, using Judd–Ofelt theory [7, 8]. The MD contribution can be calculated from first principles. Both contributions are independent of temperature.

The vibronic process results in side bands accompanying the zero-phonon line; the side bands are shifted by a frequency ω_i from the zero-phonon line, where ω_i is one of the vibrational frequencies of the lattice. We can write the vibronic transition rate at 0 K as

$$A_{vib}(0) = \sum_i A^i_{vib}(0) \tag{3}$$

where $A^i_{vib}(0)$ is the decay rate into the side bands at frequency ω_i. The summation is over all vibrational frequencies. A^i_{vib} increases with the temperature as

$$A^i_{vib}(T) = A^i_{vib}(0)(1 + 2n_i) \tag{4}$$

where n_i is the Bose–Einstein occupancy factor for phonons of frequency ω_i given by

$$n_i = \frac{1}{\exp(\hbar\omega_i/k_B T) - 1}. \tag{5}$$

The full vibronic transition rate increases with temperature as

$$A_{vib}(T) = \sum_i A^i_{vib}(T). \tag{6}$$

The non-radiative decay process between two $4f^7$ electronic levels is generally found to occur by the emission of the smallest number (p) of highest energy ($\hbar\omega_{max}$) phonons. This decay rate increases with temperature as [4, 9]

$$A_{nr}(T) = A_{nr}(0)(1 + n)^p \tag{7}$$

where

$$n = \frac{1}{\exp(\hbar\omega_{max}/k_B T) - 1}. \tag{8}$$

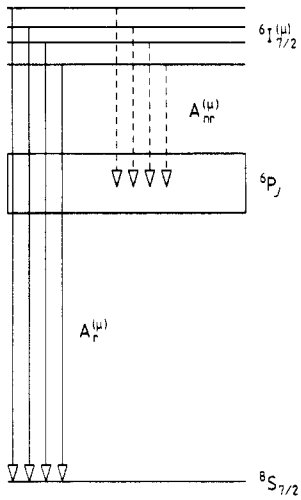

Figure 1. A schematic energy level diagram indicating the $^6I_{7/2}$ crystal field components and their different paths to lower levels. Full lines indicate radiative transitions, broken lines indicate non-radiative transitions.

To describe the decay of the $^6I_{7/2}$ term level of Gd^{3+} at low concentration in a solid, we consider the schematic picture in figure 1. In a first approximation, we neglect the crystal field splitting of the $^6I_{7/2}$ term level. The large energy difference between the first excited state ^6P_J and the ground state $^8S_{7/2}$ ($> 30\,000$ cm^{-1}) prohibits non-radiative transitions from this excited state to the ground state. Hence, for the $^6I_{7/2}$ term level the following expression holds

$$A_d(T) = A_{zp} + A_{vib}(T) + (1+n)^p A_{nr}(0) \tag{9}$$

with $A_{nr}(0)$ the total non-radiative transition rate of the $^6I_{7/2} \rightarrow {}^6P_J$ ($J = \frac{3}{2}, \frac{5}{2}, \frac{7}{2}$) transitions at 0 K.

When the crystal field splitting of the $^6I_{7/2}$ term level is taken into account, equation (9) must be modified. We note that the crystal field splitting is much smaller than the energy difference between $^6I_{7/2}$ and ^6P_J. At low temperatures only the lowest crystal field component is occupied and the variables in equation (9) must be assigned to $A_\alpha^{(1)}$, where the superscript (1) denotes the lowest component and the subscript α the various transition rates. With rising temperature, the other crystal field components are also populated and we assume a Boltzmann distribution of population among these components. The contribution of the various crystal field components to the total transition rate of the $^6I_{7/2}$ level, $A_d(T)$, may be different.

If we label the transition rates of the different crystal field components by μ, then

$$A_d(T) = \sum_\mu \exp\left(\frac{-\Delta E^{(\mu 1)}}{k_B T}\right)[A_{zp}^{(\mu)} + A_{vib}^{(\mu)}(T) + (1+n)^p A_{nr}^{(\mu)}(0)] \times \left[\sum_\mu \exp\left(\frac{-\Delta E^{(\mu 1)}}{k_B T}\right)\right]^{-1} \tag{10}$$

i.e. $A_d(T)$ is a thermal weighted summation of the transition rates of the different crystal field components. In (10), $\Delta E^{(\mu 1)}$ is the energy difference between the crystal field component labelled μ and the lowest crystal field component ($\mu = 1$).

3. Experimental details

3.1. Sample preparation

The preparation of YOCl has been described in [10]. YOCl has a structure like PbFCl; the site symmetry of the Gd^{3+} ion is C_{4v} [11].

The preparation of $LiYF_4$ has been described in [5]. $LiYF_4$ has the inverse scheelite structure. The site symmetry of the Gd^{3+} ion is S_4 [12].

The Gd^{3+} concentration in both samples was kept to about 1% in order to avoid energy migration over the Gd^{3+} sublattice.

3.2. Equipment

The laser system used to perform the measurements has been described in [13]. The only difference from the description in [14] is that we used a Spex 1269 monochromator.

4. Results and discussion

4.1. YOCl:Gd

The decay rate of the $^6I_{7/2}$ emission versus temperature is given in figure 2. It has been shown previously [10] that the $^6I_{7/2}$ term level consists of two close pairs of crystal field components, namely $^6I_{7/2}^{(1,2)}$ and $^6I_{7/2}^{(3,4)}$ (see the inset in figure 2). Excitation was into the $^6I_{7/2}^{(3,4)}$ level at 35 658 cm^{-1}. Emission was observed at 35 610 cm^{-1}, which is the $^6I_{7/2}^{(1,2)}$ level. All decay curves are exponential. The increase of the transition rate $A_d(T)$ with temperature is mainly due to the increase of the non-radiative transition rate $^6I_{7/2} \rightarrow {}^6P_J$, as argued below.

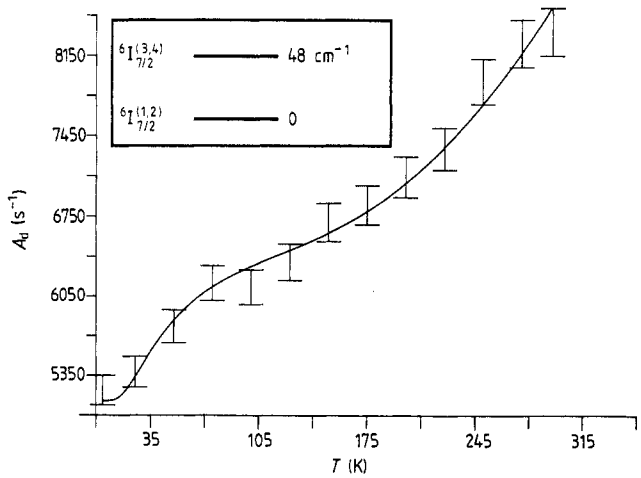

Figure 2. The temperature dependence of the total decay rate $A_d(T)$ of the $^6I_{7/2}$ level of Gd^{3+} in YOCl. The full curve is a fit discussed in the text. Inset: the energy level structure of the $^6I_{7/2}$ term level.

The temperature dependence of the decay rate of the $^6I_{7/2}$ emission can be analysed quantitatively, using the general expression (10). In the case of Gd^{3+} in YOCl, equation (10) can be simplified. The $^6I_{7/2}$ level is split into four components, but the components are grouped in two pairs. Therefore, the summation index $\mu' = (1,2), (3,4)$ is used instead of μ.

Of the transition rates required for equation (10), $A_{zp}^{(1,2)}$, $A_{vib}^{(1,2)}(0)$, and $A_{nr}^{(1,2)}(0)$ can be obtained from spectroscopic measurements at low temperatures [5, 10]. The ratio r of $A_{vib}^{(1,2)}(0)$ to $A_{zp}^{(1,2)}$ is small, $r = 0.1$ [10], while $A_{nr}^{(1,2)}$ is greater than $A_{zp}^{(1,2)}$ by a factor of about 13. Thus $A_{vib}^{(1,2)}(0)$ represents less than 1% of the decay rate of the $^6I_{7/2}^{(1,2)}$ level, and to a very good approximation we can neglect the variations with temperature of $A_{vib}^{(1,2)}$.

By raising the temperature the value of $A_{zp}^{(3,4)}$ can be found [5, 10], and we assume that the ratio of $A_{vib}^{(3,4)}$ to $A_{zp}^{(3,4)}$ is constant at the same value of r, namely $r = 0.1$. Thus $A_{nr}^{(3,4)}$ is the only unknown decay rate in (10).

If it is assumed that the non-radiative decay occurs between $^6I_{7/2}$ and $^6P_{3/2}$ (the highest ^6P_J state) then

$$p \approx \Delta E(^6I_{7/2} \leftrightarrow {}^6P_{3/2})/\hbar\omega_{max}. \tag{11}$$

The maximum phonon energy, $\hbar\omega_{max}$, equals 555 cm^{-1} [10]. The energy difference ΔE ($^6I_{7/2} \leftrightarrow {}^6P_{3/2}$) is about 2500 cm^{-1}. Hence, p is expected to be equal to 4 or 5. We note that the energy gap between $^6I_{7/2}$ and $^6P_{5/2}$ (the second highest ^6P_J state) is about 3100 cm^{-1}, corresponding to $p = 5$ or 6.

The best (Gauss–Newton) fit to (10) is obtained with $p = 4$ and is drawn in figure 2. The fit parameters are $A_{nr}^{(3,4)}$ and $\hbar\omega_{max}$. The value of $\hbar\omega_{max}$ serves as an indicator of the quality of the fit; it can be compared directly with IR and luminescence data.

Table 1. Radiative and non-radiative transition rates at 4.2 K for the crystal field components of the $^6I_{7/2}$ level of Gd^{3+} in YOCl. The radiative transitions are to the ground state $^8S_{7/2}$, the non-radiative transitions to $^6P_{3/2}$. The values of the rates of $^6I_{7/2}^{(1,2)}$, and $A_{zp}^{(3,4)}$ are revised data from [10], presented in the erratum. The value of $A_{vib}^{(3,4)}$ is estimated (see text); the value of $A_{nr}^{(3,4)}$ follows from the fit discussed in the text.

$^6I_{7/2}{}^{(\mu)}$	$A_{nr}^{(\mu)}$ (s^{-1})	$A_{zp}^{(\mu)}$ (s^{-1})	$A_{vib}^{(\mu)}$ (s^{-1})	$\Delta E^{\{(3,4)(1,2)\}}$ (cm^{-1})
(1, 2)	4730	362	36	
(3, 4)	8040	562	56	48

We find $\hbar\omega_{max} = 562$ cm^{-1}, which is in excellent agreement with the maximum phonon energy observed for the phonon side band of the $^6P_{7/2} \rightarrow {}^8S_{7/2}$ transition, namely 555 cm^{-1} [10]. With $p = 4$ and $\hbar\omega_{max} = 562$ cm^{-1}, the non-radiative transition ends at the $^6P_{3/2}$ state.

The value of $A_{nr}^{(3,4)}$ obtained from the fit is 8040 s^{-1}. In table 1, all the rates of transitions from the $^6I_{7/2}$ components are presented.

4.2. $LiYFv_4$:Gd

In an earlier publication from this group [5], the non-radiative decay rate of the $^6I_{7/2}$ level of Gd^{3+} in $LiYF_4$ was measured. It was assumed that all the crystal field levels

contribute in the same way to the non-radiative decay rate of the $^6I_{7/2}$ term level. We present here a new analysis of the data published in [5], using equation (10). This results in a better fit to the data.

The $^6I_{7/2}$ level splits into four components. The radiative and non-radiative rates of the lowest crystal field component are measured at low temperatures: $A_r^{(1)} = 48.6\ s^{-1}$ and $A_{nr}^{(1)} = 612.3$ [5]. The values for the radiative rates of the other components are calculated from the intensity ratio of the different emission lines at room temperature by using the equation

$$A_r^{(\mu)} = A_r^{(1)} \exp\left(\frac{\Delta E^{(\mu 1)}}{k_B T}\right) \frac{I(^6I_{7/2}^{(\mu)})}{I(^6I_{7/2}^{(1)})}.$$

The measured decay rate $A_d(T)$ is given in figure 3 as a function of temperature. The full curve is a fit to equation (10), with μ ranging from 1 to 4. The fit parameters are $A_{nr}^{(2)}$, $A_{nr}^{(3)}$, $A_{nr}^{(4)}$and $\hbar\omega_{max}$.

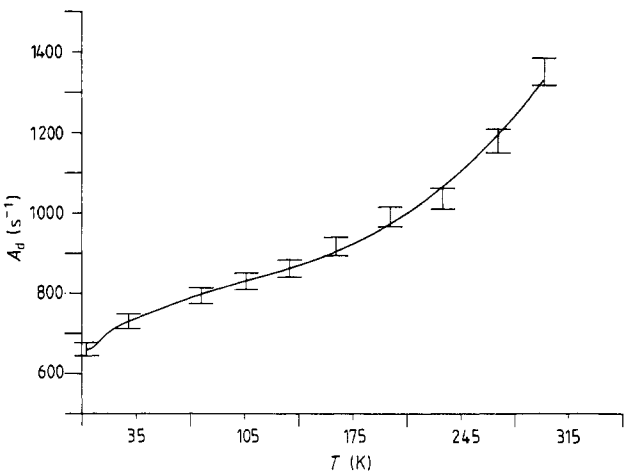

Figure 3. The temperature dependence of the total decay rate $A_d(T)$ of the $^6I_{7/2}$ level of Gd^{3+} in $LiYF_4$. The full curve is a fit discussed in the text.

Again, to estimate the zero-phonon and the vibronic transition rates, we assume that the vibronic coupling is the same for all crystal field components. The intensity ratio of the vibronic side band and the zero-phonon line of the $^6I_{7/2}^{(1)}$ component is found to be 2% [14] and this ratio is assumed for the other levels. We then have $A_{zp}^{(1)} = 47.6\ s^{-1}$; the values for $A_{zp}^{(\mu)}$ and $A_{vib}^{(\mu)}$ ($\mu = 2,3,4$) are tabulated in table 2. The values for $\Delta E^{(\mu 1)}$ [5] are also in table 2.

The most reliable fit is obtained for $p = 6$ and yields $\hbar\omega_{max} = 556\ cm^{-1}$. This energy corresponds closely to the energy of the E_u ω_{LO} phonon mode [15], which is indeed the phonon mode with the highest energy in $LiYF_4$. The fitting parameters $A_{nr}^{(\mu)}(\mu = 2,3,4)$ are presented in table 2. With $p = 6$ and $\hbar\omega_{max} = 556\ cm^{-1}$, the non-radiative transition involved is $^6I_{7/2} \rightarrow {}^6P_{5/2}$, although the energy difference is larger by about the energy of one phonon than the energy difference between the $^6I_{7/2}$ and the $^6P_{3/2}$ term levels. A fit with $p = 4$ or 5 as a constraint results in a value for $\hbar\omega_{max}$ which is not found in the IR spectrum [15].

Table 2. Radiative and non-radiative transition rates at 4.2 K for the crystal field components of the $^6I_{7/2}$ level of Gd^{3+} in $LiYF_4$. The radiative transitions are to the ground state $^8S_{7/2}$, the non-radiative transitions are to $^6P_{5/2}$.

$^6I_{7/2}{}^{(\mu)}$	$A_{nr}^{(\mu)}$ (s^{-1})	$A_{zp}^{(\mu)}$ (s^{-1})	$A_{vib}^{(\mu)}$ (s^{-1})	$\Delta E^{(\mu 1)}$ (cm^{-1})
(1)	612.3	47.6	1.0	
(2)	826.3	128.6	2.6	21
(3)	380.4	120.9	2.4	48
(4)	1460	307.4	6.2	101

4.3. Comparison of the results of YOCl:Gd and $LiYFv_4$:Gd

We observe from tables 1 and 2 that the radiative and non-radiative rates are one an order of magnitude larger for YOCl than for $LiYF_4$. The matrix element of the MD operator between $^6I_{7/2}$ and $^8S_{7/2}$ is negligible [16], hence the radiative transitions from the $^6I_{7/2}$ term level proceed essentially through the FED process.

The site symmetry of Gd^{3+} in YOCl is C_{4v}; in $LiYF_4$ the Gd^{3+} site is a deformed cubic site with S_4 symmetry. The former site lacks inversion symmetry completely, the latter is not far from inversion symmetry. Further, covalency will be more pronounced in the oxychloride than in the fluoride. This implies a much stronger mixing, by odd-parity crystal field components and/or a ligand polarisation mechanism [17], of opposite-parity states into the $4f^7$ wave functions of Gd^{3+} in YOCl. This mixing allows FED transitions to occur. Consequently $A_r(YOCl) > A_r(LiYF_4)$, where A_r represents the radiative rate of decay to the ground state. With the same argument, radiative rates between two excited RE levels will be larger in YOCl than in $LiYF_4$. Van Dijk and Schuurmans have shown that the ED radiative and non-radiative rates, belonging to a transition between two RE levels, are proportional [18]. Therefore we may expect that for non-radiative transitions between two excited levels $A_{nr}(YOCl) > A_{nr}(LiYF_4)$, as observed. (Non-radiative transitions to the ground state do not occur in Gd^{3+}.)

Since the non-radiative decay rates between two $4f^7$ levels are generally found to decrease significantly if the gap between the levels increases [19], one would expect that the $^6I_{7/2} \rightarrow {}^6P_{3/2}$ decay, which is across the smallest gap (4–5 phonons), would dominate the non-radiative decay from the $^6I_{7/2}$ term level. The next largest gap (5–6 phonons) occurs for $^6I_{7/2} \rightarrow {}^6P_{5/2}$. From the fits to the data (figures 2 and 3) we find that this non-radiative decay for Gd^{3+} in YOCl is a four-phonon process, indicative of a $^6I_{7/2} \rightarrow {}^6P_{3/2}$ transition, while for Gd^{3+} in $LiYF_4$ the decay is a six-phonon process, indicating a $^6I_{7/2} \rightarrow {}^6P_{5/2}$ transition across the larger gap.

To seek an explanation for the predominance of the six-phonon relaxation process for Gd^{3+} in $LiYF_4$, we consider the relative sizes of the ED matrix elements for the radiative transitions. As van Dijk and Schuurmans have shown this matrix element is proportional to the matrix element of the ion–lattice coupling for the non-radiative transition. The proportionality factor will be larger in YOCl:Gd^{3+}because of the low point symmetry of the Gd^{3+} site and the larger value of the polarisability α [18]. From the analysis of Judd and Ofelt [7, 8] we find that the ED matrix element depends on the product of the parameters Ω_λ and the square of the unit tensor operators $U^{(\lambda)}$, with $\lambda = 2, 4, 6$. Values of $(U^{(\lambda)})^2$ are negligibly small for the $^6I_{7/2} \rightarrow {}^6P_{3/2}$ transition, while for $^6I_{7/2} \rightarrow {}^6P_{5/2}$ we find $(U^{(6)})^2 = 0.70$ [20]. Thus the coupling matrix element is

much larger for the transition to the $^6P_{5/2}$ term level, which allows this transition to be the dominant relaxation process of the $^6I_{7/2}$ term level in $LiYF_4$. For Gd^{3+} in YOCl a non-negligible ED matrix element for the $^6I_{7/2} \rightarrow {}^6P_{3/2}$ transition is obtained, due to the larger values of A_{zp} and, therefore, of Ω_λ(YOCl). This makes the four-phonon process the dominant relaxation process of the $^6I_{7/2}$ term level in YOCl.

For Gd^{3+} in a borate glass, for which $\hbar\omega_{max} \approx 1400\ cm^{-1}$, only two phonons are required to make the $^6I_{7/2} \rightarrow {}^6P_J$ transition. For this material the non-radiative rate is so large that no luminescence is observed from the $^6I_{7/2}$ term level [21]. In general, the non-radiative rate increases with decreasing number of phonons required [9]. The occurrence of the six-phonon process in $LiYF_4$:Gd is, therefore, another reason why $A_{nr}(YOCl) > A_{nr}(LiYF_4)$.

In conclusion, we have analysed the temperature dependence of the decay rate of the $^6I_{7/2}$ level of Gd^{3+} in YOCl and $LiYF_4$. The decay is described as a thermal-weighted average of the contributions of the different crystal field components of the $^6I_{7/2}$ level. All rates are larger in YOCl than in $LiYF_4$.

Acknowledgments

GFI wishes to thank the University of Utrecht for a temporary appointment as visiting professor (F C Donders chair). The investigations were partly supported by the Netherlands Foundation of Chemical Research (SON) with financial aid from the Netherlands Foundation for the Advancement of Pure Research (NWO) and the Netherlands Foundation for Technical Research.

References

[1] Blasse G 1987 *Mater. Chem. Phys.* **16** 201
[2] Blasse G 1989 *Chem. Mater.* **1** 294
[3] Weber M J 1979 *Handbook on the Physics and Chemistry of Rare Earths* vol 4, ed K A Gschneider Jr and L R Eyring (Amsterdam: North-Holland) ch 35
[4] Di Bartolo B (ed) 1980 *Radiationless Processes* (New York: Plenum); 1990 *Advances in Nonradiative Processes in Solids* (New York: Plenum) at press
[5] de Vries A J, Hazenkamp M F and Blasse G 1988 *J. Lumin.* **42** 275
[6] Di Bartolo B (ed) 1983 *Energy Transfer Processes in Condensed Matter* (New York: Plenum)
[7] Judd B R 1962 *Phys. Rev.* **127** 750
[8] Ofelt G S 1962 *J. Chem. Phys.* **37** 339
[9] Reisfeld R and Jørgensen C K 1977 *Lasers and Excited States of Rare Earths* (Berlin: Springer) ch 2
[10] Sytsma J, Imbusch G F and Blasse G 1989 *J. Chem. Phys.* **91** 1456 (An erratum to this paper will appear in 1990 *J. Chem. Phys.* **92** 3249)
[11] Wyckoff R W G 1961 *Crystal Structures* vol 1 (New York: Wiley)
[12] Burns J H 1965 *Inorg. Chem.* **4** 881
[13] de Vries A J, van Vliet J P M and Blasse G 1988 *Phys. Status Solidi* b **149** 391
[14] Sytsma J, van Schaik W and Blasse G to be published
[15] Miller S A, Rast H E and Caspers H H 1970 *J. Chem. Phys.* **52** 4172
[16] Detrio J A 1971 *Phys. Rev.* B **4** 1422
[17] Mason S F and Tranter G E 1983 *Chem. Phys. Lett.* **94** 29
[18] van Dijk J M F and Schuurmans M F H 1983 *J. Chem. Phys.* **78** 5317
[19] Riseberg L A and Weber M J 1976 *Progress in Optics* vol 14, ed E Wolf (Amsterdam: North-Holland) p 89
[20] Carnall W T, Crosswhite H and Crosswhite H M 1977 Energy level structure and transition probabilities of the trivalent lanthanides in LaF_3 *Argonne National Laboratory Report*
[21] Verweij J W M 1989 private communication